Inorg. Chem. **2008**, *47*, 7415−7423

Mixed-Ligand Uranyl(V) β-Diketiminate/β-Diketonate Complexes: Synthesis and Characterization

Trevor W. Hayton* and Guang Wu

Department of Chemistry and Biochemistry, University of California, Santa Barbara, Santa Barbara, California 93106

Received April 29, 2008

The reaction of $[UO_2(Ar_2nacnac)Cl]_2$ [$Ar_2nacnac$ = (2,6-$^iPr_2C_6H_3$)NC(Me)CHC(Me)N(2,6-$^iPr_2C_6H_3$)] with Na(RC(O)CHC(O)R) (R = Me, Ph, CF_3) in tetrahydrofuran results in the formation of $UO_2(Ar_2nacnac)(RC(O)CHC(O)R)$ (R = Me, **1**; Ph, **2**; CF_3, **3**), which can be isolated in moderate yields. The structures of **1** and **2** have been confirmed by X-ray crystallography, while the solution redox properties of **1**−**3** have been measured by cyclic voltammetry. Complexes **1**−**3** exhibit reduction features at −1.82, −1.59, and −1.39 V (vs Fc/Fc^+), respectively, at a scan rate of 100 $mV \cdot s^{-1}$. The decrease in the reduction potential follows the electron-withdrawing ability of each β-diketonate ligand. Chemical reduction of **1** and **2** with Cp^*_2Co in toluene yields $[Cp^*_2Co][UO_2(Ar_2nacnac)(RC(O)CHC(O)R)]$ (R = Me, **4**; Ph, **5**), while reduction of **3** with Cp_2Co provides $[Cp_2Co][UO_2(Ar_2nacnac)(CF_3C(O)CHC(O)CF_3)]$ (**6**). Complexes **4**−**6** have been fully characterized, while the solid-state molecular structure of **5** has also been determined. In contrast to the clean reduction that occurs with Cp^*_2Co, reduction of **1** with sodium ribbon, followed by cation exchange with $[NEt_4]Cl$, produces $[NEt_4][UO_2(Ar_2nacnac)(H_2C{=}C(O)CH(O)CMe)]$ (**7**) in modest yield. This product results from the formal loss of $H^\bullet$ from a methyl group of the acetylacetonate ligand. Alternately, complex **7** can be synthesized by deprotonation of **1** with $NaNTMS_2$ in good yield.

Introduction

Understanding the chemistry of the actinyl ions, AnO_2^{n+} (where An = U, Np, Pu; n = 1, 2), has wide-ranging consequences for nuclear fuel processing, waste treatment, and environmental remediation.[1] One of these ions ($U^VO_2^+$) is also of interest because of its intermediacy in the photochemical reactivity of uranyl(VI), which has been suggested as a catalyst for solar energy storage.[2,3] In addition, $U^VO_2^+$ is a likely intermediate in the reduction of UO_2^{2+} to uranyl(IV), by biotic and abiotic means.[4,5] This fragment is also isostructural with the neptunyl(V) ion. $Np^VO_2^+$ has proven difficult to extract from spent nuclear fuel using current processing technologies[1,6,7] and exhibits appreciable mobility in groundwater, which is a concern for the long-term geological storage of this element.[8,9] However, the ability to draw parallels between these two actinyl ions has, until quite recently, been limited by the lack of suitable $U^VO_2^+$ complexes.

The uranyl(V) ion was first studied during the 1940s[10–13] and has been the subject of numerous investigations since, but relative to the uranyl(VI) ion, very little is known about $U^VO_2^+$. Uranyl(V) can be conveniently generated by pho-

* To whom correspondence should be addressed. E-mail: hayton@chem.ucsb.edu.

(1) Katz, J. J.; Seaborg, G. T.; Morss, L. R. *The Chemistry of the Actinide Elements*, 2nd ed.; Chapman and Hall: New York, 1986; Vol. *1*.
(2) Jørgensen, C. K.; Reisfeld, R. *J. Electrochem. Soc.* **1983**, 681–684.
(3) Jørgensen, C. K.; Reisfeld, R. *Struct. Bonding (Berlin)* **1982**, *50*, 121–172.
(4) Renshaw, J. C.; Butchins, L. J. C.; Livens, F. R.; May, I.; Charnock, J. M.; Lloyd, J. R. *Environ. Sci. Technol.* **2005**, *39*, 5657–5660.
(5) Ilton, E. S.; Haiduc, A.; Cahill, C. L.; Felmy, A. R. *Inorg. Chem.* **2005**, *44*, 2986–2988.
(6) Tian, G.; Xu, J.; Rao, L. *Angew. Chem., Int. Ed.* **2005**, *44*, 6200–6203.
(7) Tian, G.; Zhang, P.; Wang, J.; Rao, L. *Solvent Extr. Ion. Exch.* **2005**, *23*, 631–643.
(8) Gorden, A. E. V.; Xu, J.; Raymond, K. N.; Durbin, P. *Chem. Rev.* **2003**, *103*, 4207–4282.
(9) Kaszuba, J. P.; Runde, W. H. *Environ. Sci. Technol.* **1999**, *33*, 4427–4433.
(10) Harris, W. E.; Kolthoff, I. M. *J. Am. Chem. Soc.* **1945**, *67*, 1484–1490.
(11) Kern, D. M. H.; Orlemann, E. F. *J. Am. Chem. Soc.* **1949**, *71*, 2102–2106.
(12) Kolthoff, I. M.; Harris, W. E. *J. Am. Chem. Soc.* **1946**, *68*, 1175–1179.
(13) Heal, H. G. *Nature* **1946**, *157*, 225.

10.1021/ic800778j CCC: $40.75
Published on Web 07/17/2008

tolysis of uranyl (UO_2^{2+}) in the presence of alcohols or alkanes,[14–24] or it can be synthesized electrochemically.[19,25–34] However, it has never been isolated in the solid state when made by either of these methods, in part because of its facile disproportionation to UO_2^{2+} and U^{4+}.[35] Only recently has a synthetic approach to isolable uranyl(V) been developed. For instance, it can be generated in good yield by the oxidation of $UI_3(THF)_4$ with pyridine *N*-oxide under anhydrous conditions, where it is isolated as a 1D coordination polymer, $\{[UO_2(py)_5][KI_2(py)_2]\}_n$.[36] This same material can also be formed by the reduction of $UO_2I_2(THF)_3$ with KC_5Me_5.[37] In addition, our laboratory has recently isolated $UO_2(Ar_2nacnac)(Ph_2MePO)_2$, in reasonable yield.[38]

We are continuing to explore the ability of the β-diketiminate class of ligands to stabilize the uranyl(V) fragment.[38] The β-diketiminate ligands were chosen because of their bulky aryl substituents, which are oriented parallel to the O═U═O vector, should effectively block dimerization by providing steric protection for the two oxo ligands and subsequently slow the disproportionation reaction. However, our previously isolated uranyl(V) complex, $UO_2(Ar_2nacnac)(Ph_2MePO)_2$, rapidly decomposes in CH_2Cl_2 and undergoes ligand exchange with tetrahydrofuran (THF). The facile loss of Ph_2MePO from this complex likely explains its observed instability. As a result, we have endeavored to find bidentate coligands to complement the $Ar_2nacnac$ fragment and have chosen to investigate the β-diketonate class of ligands to establish their capacity for stabilizing $U^VO_2^+$. The bidentate β-diketonates should be less likely to undergo ligand exchange than a monodentate ligand set, thus providing the desired kinetic stabilization to the uranyl(V) moiety. In addition, the β-diketonates offer the capacity to modulate the redox potential of the uranium center by changing the substituents of the ligand backbone. This affords the ability to examine how the redox potential, and the substituents themselves, can affect the stability of the resulting uranyl(V) complexes.

A few uranyl(V) β-diketonates have been previously reported. For instance, in situ reduction of $UO_2(dbm)_2(DMSO)$ leads to the formation of $[UO_2(dbm)_2(DMSO)]^-$, which can be observed spectroscopically,[32,34] while the solid-state molecular structure of $\{[UO_2(dbm)_2]_4[K_6(py)_{10}]\}^{2+}$, a tetrameric $U^VO_2^+$ complex held together by bridging uranyl−oxo interactions, was recently determined.[39]

Results and Discussion

The reaction of $[UO_2(Ar_2nacnac)Cl]_2$ with 2 equiv of Na(acac) [acac = MeC(O)CHC(O)Me] in THF results in a rapid color change to deep red and the formation of $UO_2(Ar_2nacnac)(acac)$ (**1**), which can be isolated in 42% yield as a dark crystalline solid (eq 1). Similarly, the reaction of $[UO_2(Ar_2nacnac)Cl]_2$ with Na(dbm) [dbm = dibenzoylmethanate, PhC(O)CHC(O)Ph] and Na(hfac) [hfac = hexafluoroacetylacetonate, $CF_3C(O)CHC(O)CF_3$] provides $UO_2(Ar_2nacnac)(dbm)$ (**2**) and $UO_2(Ar_2nacnac)(hfac)$ (**3**), respectively, in moderate yields.

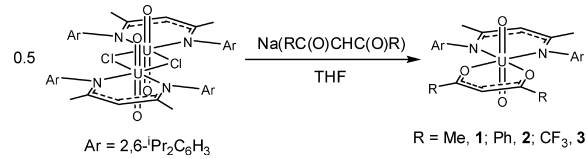

(1)

Complexes **1**−**3** are readily soluble in Et_2O, toluene, and THF and somewhat soluble in hexanes. The ^1H NMR spectrum of **1** in C_6D_6 exhibits singlets at 1.64 and 4.98 ppm, in a ratio of 6:1, indicating the inclusion of the acac ligand into the uranyl coordination sphere. The ^1H NMR spectrum of **2** in C_6D_6 exhibits a singlet at 6.72 ppm, assignable to the γ proton of the dbm ligand, and a doublet at 7.66 ppm, assignable to the ortho protons of the dbm phenyl substituents, while complex **3** exhibits a singlet in its $^{19}F\{^1H\}$ NMR spectrum at −12.7 ppm, assignable to the CF_3 groups of the hfac ligand, and a singlet in its ^1H NMR spectrum at 6.06 ppm, assignable to the γ proton of hfac.

The UV/vis spectrum of **1** in CH_2Cl_2 consists of an absorption at 595 nm (ε = 330 L·mol^{-1}·cm^{-1}) and an absorption at 444 nm (ε = 640 L·mol^{-1}·cm^{-1}) and is qualitatively similar to the spectrum of $[UO_2(Ar_2nacnac)Cl]_2$.[38] As with the UV/vis spectrum of $[UO_2(Ar_2nacnac)Cl]_2$, we have been unable to determine which absorption is due to the UO_2^{2+} chromophore (typically

(14) Nagaishi, R.; Katsumura, Y.; Ishigure, K.; Aoyagi, H.; Yoshida, Z.; Kimura, T.; Kato, Y. *J. Photochem. Photobiol. A* **2002**, *146*, 157–161.
(15) Howes, K. R.; Bakac, A.; Espenson, J. H. *Inorg. Chem.* **1988**, *27*, 791–794.
(16) Wang, W. D.; Bakac, A.; Espenson, J. H. *Inorg. Chem.* **1995**, *34*, 6034–6039.
(17) Waltz, W. L.; Lilie, J.; Xu, X.; Sedlák, P.; Möckel, H. *Inorg. Chim. Acta* **1999**, *285*, 322–325.
(18) Bell, J. T.; Buxton, S. R. *J. Inorg. Nucl. Chem.* **1974**, *36*, 1575–1579.
(19) Mizuoka, K.; Ikeda, Y. *Inorg. Chem.* **2003**, *42*, 3396–3398.
(20) Miyake, C.; Yamana, Y.; Imoto, S.; Ohya-Nishiguchi, H. *Inorg. Chim. Acta* **1984**, *95*, 17–21.
(21) Miyake, C.; Yamana, Y.; Imoto, S. *Inorg. Chim. Acta* **1984**, *94*, 11–12.
(22) Miyake, C.; Sano, Y. *J. Alloys Compd.* **1994**, *213/214*, 493–496.
(23) Mao, Y.; Bakac, A. *J. Phys. Chem.* **1996**, *100*, 4219–4223.
(24) Mao, Y.; Bakac, A. *Inorg. Chem.* **1996**, *35*, 3925–3930.
(25) Kim, S.-Y.; Asakura, T.; Morita, Y.; Ikeda, Y. *J. Alloys Compd.* **2006**, *408−412*, 1291–1295.
(26) Ferri, D.; Grenthe, I.; Salvatore, F. *Inorg. Chem.* **1983**, *22*, 3162–3165.
(27) Cohen, D. *J. Inorg. Nucl. Chem.* **1970**, *32*, 3525–3530.
(28) Ikeda, A.; Hennig, C.; Tsushima, S.; Takao, K.; Ikeda, Y.; Scheinost, A. C.; Bernhard, G. *Inorg. Chem.* **2007**, *46*, 4212–4219.
(29) Docrat, T. I.; Mosselmans, J. F. W.; Charnock, J. M.; Whiteley, M. W.; Collison, D.; Livens, F. R.; Jones, C.; Edminston, M. J. *Inorg. Chem.* **1999**, *38*, 1879–1822.
(30) Bell, J. T.; Friedman, H. A.; Billings, M. R. *J. Inorg. Nucl. Chem.* **1974**, *36*, 2563–2567.
(31) Mizuoka, K.; Grenthe, I.; Ikeda, Y. *Inorg. Chem.* **2005**, *44*, 4472–4474.
(32) Mizuoka, K.; Ikeda, Y. *Radiochim. Acta* **2004**, *92*, 631–635.
(33) Shirasaki, K.; Yamamura, T.; Shiokawa, Y. *J. Alloys Compd.* **2006**, *408−412*, 1296–1301.
(34) Mizuoka, K.; Tsushima, S.; Hasegawa, M.; Hoshi, T.; Ikeda, Y. *Inorg. Chem.* **2005**, *44*, 6211–6218.
(35) Ekstrom, A. *Inorg. Chem.* **1974**, *13*, 2237–2241.
(36) Natrajan, L.; Burdet, F.; Pécaut, J.; Mazzanti, M. *J. Am. Chem. Soc.* **2006**, *128*, 7152–7153.
(37) Berthet, J.-C.; Siffredi, G.; Thuéry, P.; Ephritikhine, M. *Chem. Commun.* **2006**, 3184–3186.
(38) Hayton, T. W.; Wu, G. *J. Am. Chem. Soc.* **2008**, *130*, 2005–2014.
(39) Burdet, F.; Pecaut, J.; Mazzanti, M. *J. Am. Chem. Soc.* **2006**, *128*, 16512–16513.

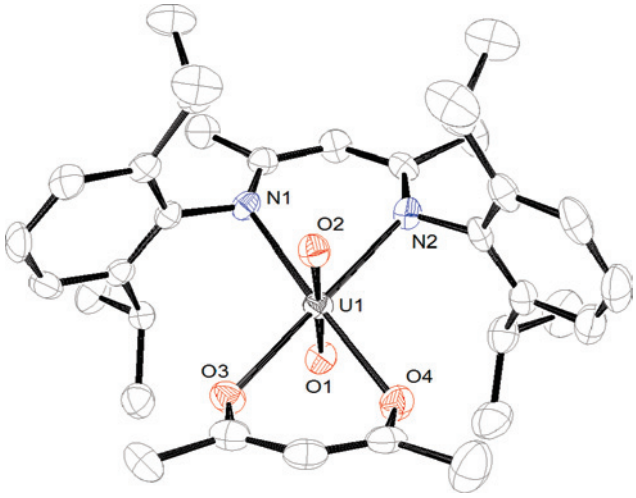

Figure 1. Solid-state molecular structure of **1**. Selected bond lengths (Å) and angles (deg): U1−O1 = 1.773(4), U1−O2 = 1.774(4), U1−O3 = 2.321(4), U1−O4 = 2.314(5), U1−N1 = 2.419(5), U1−N2 = 2.409(5), O1−U1−O2 = 178.4(2), O3−U1−O4 = 73.5(2), N1−U1−N2 = 71.5(2).

observed at 415 nm).[40] The room-temperature emission spectrum of **1** reveals a peak centered at 371 nm (λ_{ex} = 300 nm). Interestingly, no emission is observed upon excitation at 415 nm. Complexes **2** and **3** exhibit absorptions in the visible region at 609 nm (ε = 470 L·mol^{-1}·cm^{-1}) and 680 nm (ε = 580 L·mol^{-1}·cm^{-1}), respectively. Again, we could not assign an absorption to the uranyl chromophore for these two species.

The IR spectrum of **1** as a KBr pellet exhibits a strong peak at 933 cm^{-1}, which we have assigned to the U=O asymmetric stretch. Similarly, the IR spectrum of **3** as a KBr pellet exhibits a strong peak at 922 cm^{-1}, which we have also assigned to ν_{asy}(U=O). However, no vibration in the IR spectrum of **2** could confidently be assigned to this mode. The values observed for **1** and **3** are in the range of other uranyl complexes, including $UO_2I_2(THF)_3$ (928 cm^{-1}) and $UO_2(OTf)_2(py)_3$ (943 cm^{-1}).[41,42]

Crystals of **1** suitable for X-ray diffraction analysis were grown from a hexanes solution stored at −25 °C. Complex **1** crystallizes in the monoclinic space group $P2_1/c$, and its solid-state molecular structure is shown in Figure 1. Complex **1** exhibits a distorted octahedral geometry with U−O(oxo) bond lengths [U1−O1 = 1.773(4) Å; U1−O2 = 1.774(4) Å] and a O1−U1−O2 angle [178.4(2)°] that are typical of the uranyl fragment. The U−O(acac) bond lengths are U1−O3 = 2.321(4) Å and U1−O4 = 2.314(5) Å, which match those reported for other uranyl β-diketonate complexes,[43,44] while the U−N bond lengths [U1−N1 = 2.419(5) Å; U1−N2 = 2.409(5) Å] agree with the values observed in previously determined uranyl β-diketiminate complexes.[38] The aryl substituents of the β-diketiminate ligand lie orthogonal to the uranyl equatorial plane, and each aryl group is tilted toward the uranium center, resulting in an average U−C(ipso) distance of 3.04 Å. The resulting steric profile along the equatorial plane is quite bulky and probably prevents further coordination to the uranyl center. This contrasts with the behavior of most bis(β-diketonate) complexes of uranyl, where a monodentate ligand (often solvent) is frequently also coordinated to the uranium center, generating a pentagonal-bipyramidal geometry.[43–45]

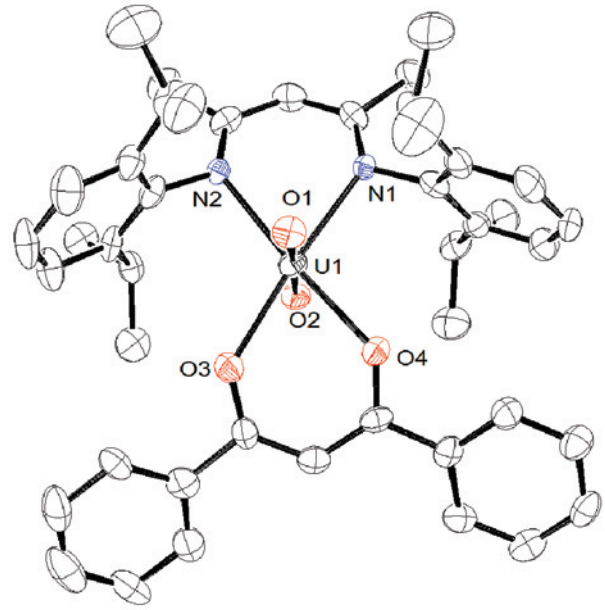

Figure 2. Solid-state molecular structure of **2**. Selected bond lengths (Å) and angles (deg): U1−O1 = 1.780(4), U1−O2 = 1.790(4), U1−O4 = 2.306(4), U1−O3 = 2.322(5), U1−N1 = 2.402(5), U1−N2 = 2.388(5), O1−U1−O2 = 178.6(2), O3−U1−O4 = 72.8(2), N1−U1−N2 = 71.6(2).

Complex **2** also crystallizes in the monoclinic space group $P2_1/c$ as a hexane solvate, **2**·C_6H_{14}. Its solid-state molecular structure is shown in Figure 2. Complex **2** exhibits a distorted octahedral geometry with U−O and U−N bond lengths similar to those observed in complex **1** [U1−N1 = 2.402(5) Å; U1−N2 = 2.388(5) Å; U1−O4 = 2.306(4) Å; U1−O3 = 2.322(5) Å]. The metrical parameters of the uranyl moiety are also comparable to those of **1** [U1−O1 = 1.780(4) Å; U1−O2 = 1.790(4) Å; O1−U1−O2 = 178.6(2)°]. In addition, the aryl groups of the diketiminate ligand are orthogonal to the uranyl equatorial plane, and the average U−C(ipso) distance is also 3.04 Å.

The solution redox properties of **1**−**3** have been investigated by cyclic voltammmetry. The cyclic voltammogram of complex **1** reveals a reduction feature at −1.82 V and an oxidation feature at −1.33 V, at a scan rate of 100 mV·s^{-1} (vs Fc/Fc$^+$), which we attribute to the UO_2^{2+}/UO_2^+ redox couple (Figure 3). Because ΔE_p is quite large (0.50 V at 100 mV·s^{-1}) and increases with increasing scan rate (Table 1), it is likely that the redox properties of **1** are affected by slow electron-transfer kinetics. Similar behavior has also been

(40) Baird, C. P.; Kemp, T. J. *Prog. React. Kinet.* **1997**, *22*, 87–139.
(41) Berthet, J.-C.; Nierlich, M.; Ephritikhine, M. *Dalton Trans.* **2004**, 2814–2821.
(42) Berthet, J.-C.; Nierlich, M.; Ephritikhine, M. *Chem. Commun.* **2004**, 870–871.
(43) Taylor, J. C.; McLaren, A. B. *Dalton Trans.* **1979**, 460–464.
(44) Kannan, S.; Rajalakshmi, N.; Chetty, K. V.; Venugopal, V.; Drew, M. G. B. *Polyhedron* **2004**, *23*, 1527–1533.
(45) Alcock, N. W.; Flanders, D. J.; Brown, D. *Dalton Trans.* **1984**, 679–681.

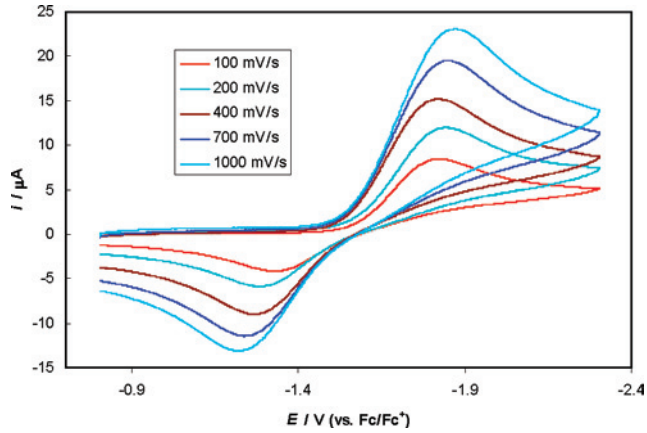

Figure 3. Room-temperature cyclic voltammogram for **1** in CH_2Cl_2 (0.1 M $[NBu_4][PF_6]$ as the supporting electrolyte).

Table 1. Summary of Electrochemical Data for Complexes **1**−**3** (vs Fc/Fc^+) in CH_2Cl_2

compound	scan rate, $V \cdot s^{-1}$	$E_{p,c}$, V	ΔE_p,[a] V
1	0.1	−1.82	0.50
	0.2	−1.84	0.56
	0.5	−1.83	0.58
2	0.1	−1.65	0.12
	0.2	−1.66	0.14
	0.5	−1.68	0.17
3	0.1	−1.39	0.30
	0.2	−1.43	0.36
	0.5	−1.47	0.45

[a] ΔE_p is defined as the potential difference between the cathodic wave and the anodic wave generated after the change in the scan direction.

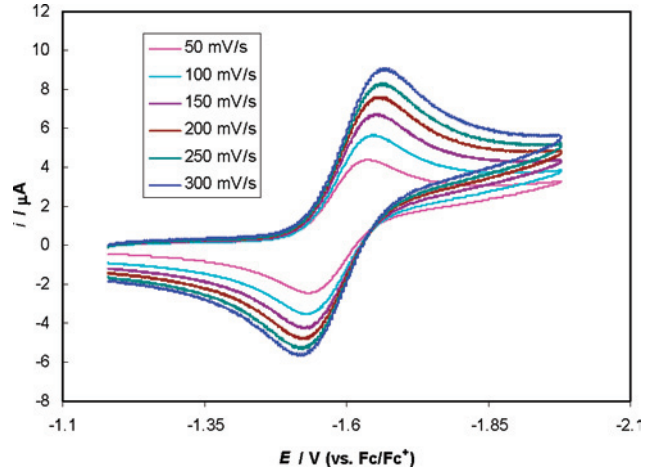

Figure 4. Room-temperature cyclic voltammogram for **2** in CH_2Cl_2 (0.1 M $[NBu_4][PF_6]$ as the supporting electrolyte).

observed in the cyclic voltammogram of $[UO_2(CO_3)_3]^{4-}$ in an aqueous solution.[46]

The cyclic voltammogram of complex **2** reveals a reversible redox feature ($E_{1/2} = -1.59$ V, vs Fc/Fc^+), as evidenced by the presence of both cathodic and anodic waves in the cyclic voltammogram (Figure 4), which we attribute to the UO_2^{2+}/UO_2^+ redox couple. In addition, $i_{p,c}/i_{p,a}$ is nearly unity, establishing its chemical reversibility, while plots of $i_{p,c}$vs $\sqrt{v}$ are linear, indicating that the oxidation is diffusion-controlled.

The cyclic voltammogram of complex **3** is similar to that observed for **1** (see the Supporting Information). It reveals a reduction feature at −1.39 V and an oxidation feature at −1.09 V, at a scan rate of 100 $mV \cdot s^{-1}$ (vs Fc/Fc^+). At this scan rate, $\Delta E_p = 0.30$ V, while at a scan rate of 0.5 $V \cdot s^{-1}$, $\Delta E_p = 0.45$ V. Because ΔE_p deviates so far from the ideal for a reversible redox couple and is dependent on the scan rate, it likely that redox properties of **3** are also affected by slow electron-transfer kinetics. In addition, complexes **1**−**3** each exhibit irreversible oxidation features at 0.55, 0.44, and 0.65 V, respectively (vs Fc/Fc^+), at a scan rate of 100 $mV \cdot s^{-1}$, which we attribute to oxidation of the uranyl coligands. A summary of relevant electrochemical data for complexes **1**−**3** is presented in Table 1.

Interestingly, we see a steady decrease of $E_{p,c}$ upon substitution of the methyl substituents of acetylacetonate with phenyl and trifluoromethyl groups (Table 1). This nicely matches the electron-withdrawing ability of each β-diketonate ligand. The potentials observed for **1**−**3** are generally in line with the UO_2^{2+}/UO_2^+ redox potentials reported for other uranyl complexes.[33,34] For instance, the related dibenzoylmethanate complex $UO_2(dbm)_2(dmf)$ exhibits a uranyl(VI)/uranyl(V) couple of −1.46 V (vs Fc/Fc^+),[25] while $[UO_2(Ar_2nacnac)(Ph_2MePO)_2][OTf]$ exhibits a potential of −1.45 V (vs Fc/Fc^+).[38]

We have attempted the chemical reduction of complexes **1**−**3** in an attempt to isolate the species generated upon electron transfer. Thus, the addition of 1 equiv of decamethylcobaltocene, dissolved in Et_2O, to a toluene solution of **1** generates $[Cp^*_2Co][UO_2(Ar_2nacnac)(acac)]$ (**4**), which precipitates from the reaction mixture as an orange-red powder (eq 2). $[Cp^*_2Co][UO_2(Ar_2nacnac)(dbm)]$ (**5**) and $[Cp_2Co][UO_2(Ar_2nacnac)(hfac)]$ (**6**) can be isolated in a similar manner by the reaction of **2** and **3** with Cp^*_2Co and Cp_2Co, respectively. Notably, the smaller reduction potential of **3**, in contrast to **1** and **2**, allows for the less reducing Cp_2Co to be used in place of Cp^*_2Co. Complexes **4**−**6** are poorly soluble in hexanes, Et_2O, and toluene but moderately soluble in THF and CH_2Cl_2. The ^1H NMR spectrum of **4** in CD_2Cl_2 is consistent with the presence of the paramagnetic uranyl(V) ion as many of the resonances are broad and shifted upfield. For instance, singlets are observed at −7.96 and −5.37 ppm, which are assignable to the methyl groups on the acac and Ar_2nacnac backbones. Similarly, in the ^1H NMR spectrum of **6** in CD_2Cl_2, a broad peak at −33.9 ppm is assignable to one set of methyl resonances of the isopropyl substituents, while the $^{19}F\{^1H\}$ NMR spectrum exhibits a broad singlet at −10.1 ppm.

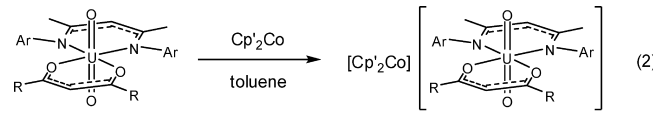

(2)

Cp' = Cp*; R = Me **4**, Ph **5**
Cp' = Cp; R = CF_3 **6**

X-ray-quality crystals of **5** were grown by allowing a 1:1 toluene/THF solution of Cp^*_2Co to slowly diffuse into a toluene solution of **2** at −25 °C. Complex **5** crystallizes in the monoclinic space group $P2_1/m$ as the toluene and THF solvate, $5 \cdot 2C_7H_8 \cdot THF$ (Figure 5). Complex **5** consists of

(46) Morris, D. E. *Inorg. Chem.* **2002**, *41*, 3542–2547.

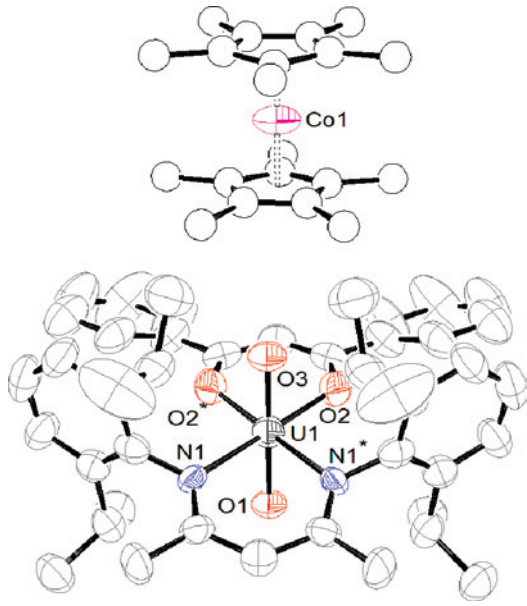

Figure 5. Solid-state molecular structure of **5**. Selected bond lengths (Å) and angles (deg): U1−O1 = 1.79(1), U1−O3 = 1.81(1), U1−O2 = 2.39(1), U1−N1 = 2.48(1), O1−U1−O3 = 179.9(6), O2−U1−O2* = 70.8(5), N1−U1−N1* = 72.6(5).

discrete cation/anion pairs: the closest intermolecular contact between the uranyl complex and the decamethylcobaltocene cation is C29−O3 = 3.4 Å. Like **2**, complex **5** possesses a distorted octahedral geometry. The U−O(oxo) bond lengths are 1.79(1) and 1.81(1) Å, and the O1−U1−O3 angle is 179.9(6)°. In addition, the U−O(dbm) and U−N bond lengths are 2.39(1) and 2.48(1) Å, respectively. Because of the low precision of the structure, the metrical parameters of the uranyl moiety in **5** are indistinguishable from those observed for **2**. However, the U−O(dbm) and U−N bond lengths in **5** are longer than those observed in **2** (by the 3σ criterion), which is consistent with the presence of the larger uranyl(V) ion.

The metrical parameters of **5** are also consistent with the theoretical predictions made for the UO_2^+ fragment and the other structurally characterized UO_2^+ complexes.[47–52] For instance, Steele and Taylor predict a U=O bond length of 1.78−1.82 Å for $[UO_2(H_2O)_5]^+$, depending on the basis set.[51] A similar prediction was also made by Hay and co-workers (1.81 Å).[49] Likewise, the experimentally determined structure of $[UO_2(Ph_3PO)_4]^+$ exhibits U−O(oxo) distances of 1.821(6) and 1.817(6) Å,[53] while the U−O(oxo) bond lengths in $UO_2(Ar_2nacnac)(Ph_2MePO)_2$ were determined to be 1.810(4) and 1.828(4) Å.[38]

The absorption spectra of complexes **4**−**6** in CH_2Cl_2 can be found in Figure 6. The spectra exhibit absorptions that

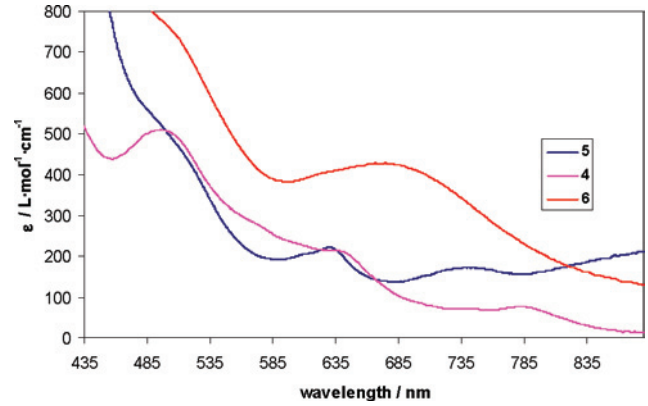

Figure 6. UV/vis spectra of **4** (2.3×10^{-3} M, pink line), **5** (1.8×10^{-3} M, blue line), and **6** (2.1×10^{-3} M, red line) in CH_2Cl_2.

are consistent with f → f transitions and the presence of a $5f^1$ ion. For instance, complex **4** exhibits transitions in the visible region, at 791 nm (ε = 75 L·mol^{-1}·cm^{-1}) and 644 nm (sh, ε = 210 L·mol^{-1}·cm^{-1}), with small molar absorptivities. Similarly, **5** exhibits peaks at 743 nm (ε = 170 L·mol^{-1}·cm^{-1}) and 634 nm (sh, ε = 220 L·mol^{-1}·cm^{-1}), and complex **6** exhibits an absorption at 677 nm (ε = 430 L·mol^{-1}·cm^{-1}). These spectra mirror that observed for $UO_2(Ar_2nacnac)(Ph_2MePO)_2$,[38] as well as several $U^VO_2^+$ complexes that were generated in situ. For instance, $[U^VO_2(CO_3)_3]^{5-}$ exhibits a weak absorption at 760 nm ($\varepsilon \sim$ 2 L·mol^{-1}·cm^{-1}), and $[U^VO_2(dbm)_2(DMSO)]^-$ exhibits a weak absorption at 640 nm ($\varepsilon \sim$ 400 L·mol^{-1}·cm^{-1}).[34]

We have also recorded the IR spectra of complexes **4**−**6** and have observed significant differences between their IR spectra and those of the uranyl(VI) analogues. For instance, in the IR spectrum of complex **4**, the asymmetric stretch of the uranyl group is assigned to the peak at 838 cm^{-1}, which is 95 cm^{-1} lower than that observed for **1**. Similarly, ν_{asy}(U=O) values for **2** and **3** are assigned to the vibrations observed at 844 and 864 cm^{-1}, respectively. These values are similar to the ν_{asy}(U=O) value reported for $UO_2(OTf)(THF)_x$ (853 cm^{-1}).[37] Moreover, the difference observed between the ν_{asy}(U=O) values for complexes **1** and **4** is consistent with previous experimental and theoretical results.[19,38,47]

The syntheses of complexes **4**−**6** take advantage of the lower solubility of the uranyl(V) anion when compared with the neutral uranyl(VI) precursor. When the reaction is performed in a solvent with relatively low polarity (such as toluene), the UO_2^+ product precipitates when formed, which greatly facilitates its isolation. In fact, when the reaction is performed in CH_2Cl_2, a UO_2^+ species is generated as expected (as determined by NMR spectroscopy), but under these conditions, no tractable material can be isolated. Not surprisingly, complexes **4**−**6** are highly air- and water-sensitive, and they are moderately temperature-sensitive. Upon standing at room temperature for 24 h, complete decomposition of the uranyl species is observed. The only identifiable product in the ^{1}H NMR spectra of these mixtures

(47) Shamov, G. A.; Schreckenbach, G.; Martin, R. L.; Hay, P. J. *Inorg. Chem.* **2008**, *47*, 1465–1475.
(48) Majumdar, D.; Balasubramanian, K.; Nitsche, H. *Chem. Phys. Lett.* **2002**, *361*, 143–151.
(49) Hay, P. J.; Martin, R. L.; Schreckenbach, G. *J. Phys. Chem. A* **2000**, *104*, 6259–6270.
(50) Gagliardi, L.; Grenthe, I.; Roos, B. O. *Inorg. Chem.* **2001**, *40*, 2976–2978.
(51) Steele, H.; Taylor, R. J. *Inorg. Chem.* **2007**, *46*, 6311–6318.
(52) Denning, R. G. *J. Phys. Chem. A* **2007**, *111*, 4125–4143.
(53) Berthet, J.-C.; Nierlich, M.; Ephritikhine, M. *Angew. Chem., Int. Ed.* **2003**, *42*, 1952–1954.

is H(Ar$_2$nacnac),[54] and we have not yet been able to identify the uranium-containing products formed upon decomposition.

We have also studied the reduction of complex **1** with other reducing agents. For instance, the reduction of **1**with sodium ribbon in THF, followed by cation exchange with [NEt$_4$]Cl, results in the formation of [NEt$_4$][UO$_2$(Ar$_2$nacnac)(H$_2$C=C(*O*)CH(*O*)CMe)] (**7**) in modest yield (eq 3). Complex **7** is a uranyl(VI) species that results from the formal loss of H$^\bullet$ from a methyl group of the acac ligand. The ^{1}H NMR spectrum of **7** is consistent with the presence of the β-diketiminate ligand in an environment where the two aryl rings are magnetically inequivalent. In addition, the signals for the two protons of the newly formed vinyl substituent are observed at 2.50 and 2.84 ppm. Each appears as a doublet (J_{HH} = 2.0 Hz).

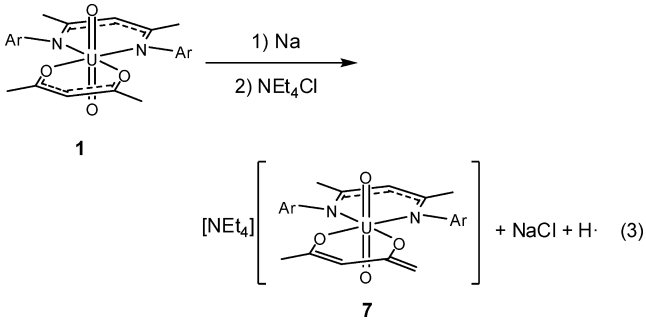

X-ray-quality crystals of **7** were grown from CH_2Cl_2/hexanes at −25 °C. Complex **7** crystallizes in the orthorhombic space group *Pnnm* as a dichloromethane solvate, **7**·2CH_2Cl_2 (Figure 7). In the solid state, complex **7** sits on a mirror plane that relates the halves of the decomposed acac ligand, rendering the vinyl and methyl substitutents indistinguishable. As such, hydrogen atoms were not assigned to these two carbon centers. However, the observed U−O bond length of the decomposed acac ligand of **7** [U1−O3 = 2.227(4) Å] is shorter than those observed for the acac ligand in **1** [U1−O3 = 2.321(4) Å; U1−O4 = 2.314(5) Å], which is consistent with the presence of a dianionic ligand and a correspondingly shorter U−O bond length. The U−O(oxo) bond lengths [U1−O1 = 1.749(7) Å; U1−O2 = 1.840(5) Å] and O−U−O angle [176.2(2)°] are within the parameters previously observed for uranyl,[1] while the U−N bond length [U1−N1 = 2.483(4) Å] is similar to those observed in **1**.

The isolation of **7** further illustrates the importance of ligand choice in stabilizing the uranyl(V) moiety. The loss of a hydrogen atom from the methyl backbone of the acac ligand probably reflects the acidity of these protons. This is also illustrated by numerous literature examples where deprotonation of the methyl groups in acac,[55] or Ar$_2$nacnac,[56–59] is facile. Given this, it is not surprising that complex **7** can also be generated by deprotonation of **1** using

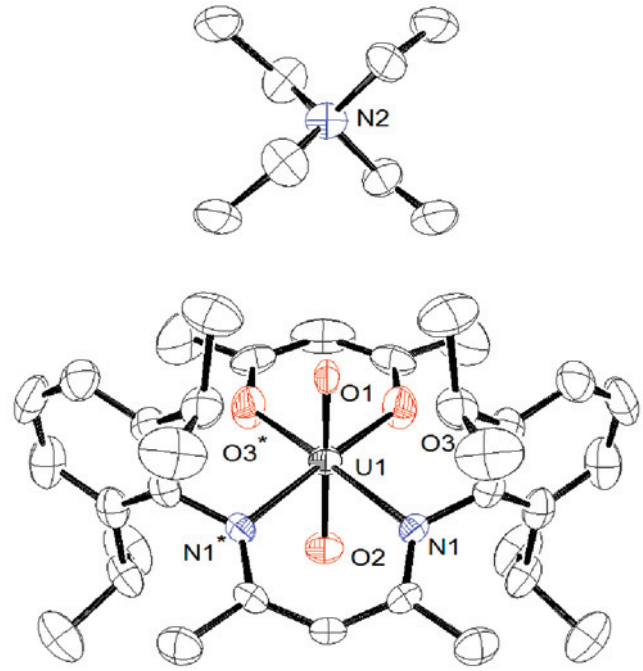

Figure 7. Solid-state molecular structure of **7**·2CH_2Cl_2. Selected bond lengths (Å) and angles (deg): U1−O1 = 1.749(7), U1−O2 = 1.840(5), U1−O3 = 2.227(4), U1−N1 = 2.483(4), O1−U1−O2 = 176.2(2), O3−U1−O3* = 76.7(2), N1−U1−N1* = 73.6(2).

a strong base (eq 4). When synthesized by this route, the isolated yield is markedly higher.

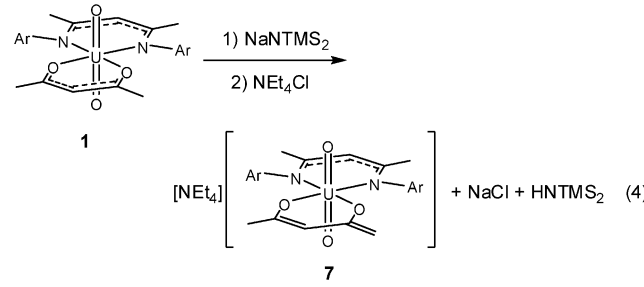

Summary

The isolation of complexes **4**−**6** is further validation of the premise that a sufficiently bulky coligand, which provides steric protection along the uranyl equatorial plane and also along the O=U=O axis, can stabilize the reactive UO_2^+ moiety. The observed stability of these complexes probably derives from the destabilization of the "cation−cation" complex (a likely intermediate during disproportionation) by the isopropyl substituents in the Ar$_2$nacnac ligand. However, the inability of these complexes to coordinate a third ligand along their equatorial plane, a result of the close U−C$_{ispo}$ interaction of the two phenyl rings and the ligation of the substitutionally inert β-diketonate to the uranyl center, probably also plays an important role in stabilization. The cyclic voltammetry results for complexes **1**−**3** illustrate the ability of the substituents on the β-diketonate coligand to

(54) Stender, M.; Wright, R. J.; Eichler, B. E.; Prust, J.; Olmstead, M. M.; Roesky, H. W.; Power, P. P. *Dalton Trans.* **2001**, 3465–3469.
(55) Clegg, W.; Horsburgh, L.; Mulvey, R. E.; Ross, M. J. *Angew. Chem., Int. Ed. Engl.* **1995**, *34*, 1233–1234.
(56) Hitchcock, P. B.; Lappert, M. F.; Protchenko, A. V. *Chem. Commun.* **2005**, 951–953.
(57) Basuli, F.; Huffman, J. C.; Mindiola, D. J. *Inorg. Chem.* **2003**, *42*, 8003–8010.
(58) Neculai, A. M.; Roesky, H. W.; Neculai, D.; Magull, J. *Organometallics* **2001**, *20*, 5501–5503.
(59) Ding, Y.; Hao, H.; Roesky, H. W.; Noltemeyer, M.; Schmidt, H. G. *Organometallics* **2001**, *20*, 4806–4811.

modulate the redox potential of the uranyl Ar_2nacnac fragment. In particular, the reduction potential can be lowered by approximately 0.4 V by switching the backbone substituents from methyl to CF_3, which allows for the less-reducing Cp_2Co to be used in place of Cp^*_2Co during the reduction to uranyl(V). The choice of the reducing agent can also effect the reaction outcome because the reduction of **1** with sodium ribbon results in ligand decomposition, as is evidenced by the isolation of **7** and not the isolation of a uranium(V) complex as intended. It is also clear from the isolation of **7**, and from the previous isolation of $UO_2(Ar_2nacnac)(CH\{Ph_2PO\}_2)$,[38] that the presence of acidic protons on the ligand set provides a potential route for uranyl(V) decomposition. Thus, care should be taken to remove any acidic substituents when designing ligand sets that are intended to stabilize UO_2^+.

Given the aforementioned importance of tailoring the uranyl ligand set by removing acidic protons, our attempts to find increasingly robust uranyl(V) derivatives will focus on ligating β-diketiminate ligands to uranyl that do not possess acidic methyl protons in their ligand backbones. Furthermore, we will also begin to explore the reactivity of the oxo ligands in these complexes, specifically to compare their Lewis basicity to that of the uranyl(VI) oxo ligands to provide further insight into the mechanism of disproportionation.

Experimental Section

General Procedures. All reactions and subsequent manipulations were performed under anaerobic and anhydrous conditions, either under high vacuum or in an atmosphere of nitrogen or argon. THF, hexanes, diethyl ether, and toluene were dried by passage over activated molecular sieves using a Vacuum Atmospheres solvent purification system. C_6D_6, CD_2Cl_2, and THF-d_8 were dried over activated 4 Å molecular sieves for 24 h before use. $[UO_2(Ar_2nacnac)Cl]_2$,[38] Na(dbm),[60] Na(acac),[61] and Na(hfac)[62] were synthesized by the published procedures. Cp^*_2Co was recrystallized from hexanes before use, while Cp_2Co was recrystallized from THF/hexanes. All other reagents were purchased from commercial suppliers and used as received.

NMR spectra were recorded on either a Varian INOVA 400 or a Varian INOVA 500 spectrometer. ^{1}H and $^{13}C\{^1H\}$ NMR spectra are referenced to external $SiMe_4$ using the residual protio solvent peaks as internal standards (^{1}H NMR experiments) or the characteristic resonances of the solvent nuclei (^{13}C NMR experiments). $^{19}F\{^1H\}$ NMR spectra were referenced to external α,α,α-trifluorotoluene. Elemental analyses were performed by the Microanalytical Laboratory at Univeristy of California at Berkeley. UV/vis spectra were recorded on a Jasco V-570 UV/vis/NIR spectrometer or an Ocean Optics USB4000 UV/vis spectrometer equipped with a USB-DT light source. Fluorescence spectra were recorded on a PTI QuantaMaster fluorimeter, and IR spectra were recorded on a Mattson Genesis FTIR spectrometer.

Cyclic Voltammetry Measurements. Cyclic voltammetry experiments were performed using a CH Instruments 600c potentiostat, and the data were processed using CHI software (version 6.29). All experiments were performed in a glovebox using a 20 mL glass vial as the cell. The working electrode consisted of a platinum disk embedded in Kel-F (2 mm diameter), the counter-electrode was a platinum wire, and the reference electrode consisted of AgCl plated on silver wire. Solutions employed during cyclic voltammetry studies were typically 3 mM in the uranium complex and 0.1 M in $[Bu_4N][PF_6]$. All potentials are reported versus the $[Cp_2Fe]^{0/+}$ couple. For all trials $i_{p,a}/i_{p,c} = 1$ for the $[Cp_2Fe]^{0/+}$ couple, while $i_{p,c}$ increased linearly with the square root of the scan rate (i.e., $\sqrt{v}$). Redox couples that exhibited behavior similar to that of the $[Cp_2Fe]^{0/+}$ couple were thus considered reversible.

$UO_2(Ar_2nacnac)(acac)$ (1). To a stirring THF solution (3 mL) containing $[UO_2(Ar_2nacnac)Cl]_2$ (0.0921 g, 0.064 mmol) was added Na(acac) (0.0156 g, 0.128 mmol). This resulted in the immediate formation of a deep-red-brown solution. After stirring for 1 h, the volatiles were removed in vacuo and the resulting oil was dissolved in toluene (3 mL). This solution was filtered through a Celite column supported on glass wool (0.5 cm × 2 cm), and toluene was then removed in vacuo. The resulting solid was rinsed with pentane (2 mL) and dried in vacuo to provide a dark-green microcrystalline powder (0.043 g, 42% yield). Anal. Calcd for $C_{34}H_{48}N_2O_4U$: C, 51.90; H, 6.15; N, 3.56. Found: C, 51.90; H, 6.01; N, 3.43. ^{1}H NMR (C_6D_6, 25 °C, 400 MHz): δ 1.09 (d, 12H, J_{HH} = 6.8 Hz, CH*Me*$_2$), 1.21 (d, 12H, J_{HH} = 6.8 Hz, CH*Me*$_2$), 1.64 (s, 6H, Me), 2.08 (s, 6H, Me), 3.79 (septet, 4H, J_{HH} = 6.8 Hz, C*H*Me$_2$), 4.98 (s, 1H), 5.06 (s, 1H), 7.28 (m, 6H, *m*- and *p*-CH). $^{13}C\{^1H\}$ NMR (C_6D_6, 25 °C, 125 MHz): δ 24.5 (CH*Me*$_2$), 26.6 (CH*Me*$_2$), 27.4 (Me), 28.1 (Me), 28.6 (C*H*Me$_2$), 98.4 (γ-C), 103.6 (γ-C), 125.4, 128.8, 137.3, 148.8 (C ipso), 167.5 (β-CN), 195.0 (β-CO). UV/vis (CH_2Cl_2, 9.92 × 10^{-4} M): 444 nm (sh, ε = 640 L·mol^{-1}·cm^{-1}), 595 nm (ε = 330 L·mol^{-1}·cm^{-1}). IR (KBr pellet, cm^{-1}): 1564(vs), 1523(vs), 1464(m), 1433(s), 1397(vs), 1361(vs), 1317(s), 1271(m), 1252(m), 1180(w), 1163(m), 1098(m), 1060(w), 1021(s), 933(s, ν_{asy}(U═O)), 908(vs), 842(w), 792(s), 756(m), 695(w), 662(w), 627(w), 545(w), 530(w), 417(m).

$UO_2(Ar_2nacnac)(dbm)$ (2). To a stirring THF solution (3 mL) containing $[UO_2(Ar_2nacnac)Cl]_2$ (0.1035 g, 0.072 mmol) was added Na(dbm) (0.0362 g, 0.15 mmol). This resulted in the immediate formation of a deep-red-brown solution. After stirring for 1 h, the volatiles were removed in vacuo and the resulting oil was dissolved in Et_2O (3 mL). This solution was filtered through a Celite column supported on glass wool (0.5 cm × 2 cm), and Et_2O was then removed in vacuo. The resulting oil was rinsed with pentane (2 mL) and dried in vacuo to provide a dark-green powder (0.0852 g, 65% yield). Recrystallization from a mixture of toluene and hexanes provides analytically pure material. Anal. Calcd for $C_{44}H_{52}N_2O_4U \cdot {}^1/_2(C_6H_{14})$: C, 59.17; H, 6.23; N, 2.94. Found: C, 59.20; H, 6.39; N, 3.18. ^{1}H NMR (C_6D_6, 25 °C, 400 MHz): δ 1.05 (d, 12H, J_{HH} = 6.8 Hz, CH*Me*$_2$), 1.21 (d, 12H, J_{HH} = 6.8 Hz, CH*Me*$_2$), 2.07 (s, 6H, Me), 3.88 (septet, 4H, J_{HH} = 6.8 Hz, C*H*Me$_2$), 5.02 (s, 1H, γ-CH), 6.72 (s, 1H, dbm γ-CH), 7.20−7.38 (m, 12H, overlapping CH), 7.66 (d, 4H, J_{HH} = 6.8 Hz, *o*-CH). $^{13}C\{^1H\}$ NMR (C_6D_6, 25 °C, 125 MHz): δ 24.7 (CH*Me*$_2$), 26.4 (CH*Me*$_2$), 27.4 (Me), 28.6 (C*H*Me$_2$), 97.2 (γ-C), 98.5 (γ-C), 125.7, 128.7, 128.8, 129.4, 132.4, 137.4, 139.6, 149.3 (C ipso), 167.8 (β-CN), 188.9 (β-CO). UV/vis (CH_2Cl_2, 3.0 × 10^{-4} M): 609 nm (ε = 470 L·mol^{-1}·cm^{-1}). UV/vis (CH_2Cl_2, 3.8 × 10^{-5} M): 397 nm (ε = 11 600 L·mol^{-1}·cm^{-1}), 331 nm (ε = 25 600 L·mol^{-1}·cm^{-1}), 292 nm (ε = 25 400 L·mol^{-1}·cm^{-1}). IR (KBr pellet, cm^{-1}): 1591(m), 1534(vs), 1522(vs), 1479(m), 1466(m), 1440(m), 1393(s), 1361(m), 1364(m), 1317(m), 1265(w), 1227(w), 1165(w), 1102(m), 1068(m), 1024(m), 935(w), 911(s), 845(w), 792(m), 756(m), 721(m), 689(m), 619(w), 607(w), 529(m), 472(m).

(60) Halcrow, M. A.; Sun, J.-S.; Huffman, J. C.; Christou, G. *Inorg. Chem.* **1995**, *34*, 4167–4177.
(61) Koiwa, T.; Masuda, Y.; Shono, J.; Kawamoto, Y.; Hoshino, Y.; Hashimoto, T.; Natarajan, K.; Shimizu, K. *Inorg. Chem.* **2004**, *43*, 6215–6223.
(62) Girolami, G. S.; Harada, Y. *Polyhedron* **2007**, *26*, 1758–1762.

Table 2. X-ray Crystallographic Data for Complexes **1**, **2**·C_6H_{14}, **5**·$2C_7H_8$·THF, and **7**·$2CH_2Cl_2$

	1	**2**·C_6H_{14}	**5**·$2C_7H_8$·THF	**7**·$2CH_2Cl_2$
empirical formula	$C_{34}H_{48}N_2O_4U$	$C_{50}H_{66}N_2O_4U$	$C_{82}H_{106}CoN_2O_5U$	$C_{44}H_{61}Cl_4N_3O_4U$
cryst habit, color	block, dark green	rod, green	irregular, orange	block, red
cryst size (mm)	0.15 × 0.15 × 0.08	0.25 × 0.10 × 0.10	0.25 × 0.15 × 0.06	0.30 × 0.20 × 0.20
cryst syst	monoclinic	monoclinic	monoclinic	orthorhombic
space group	$P2_1/c$	$P2_1/c$	$P2_1/m$	$Pnnm$
volume (Å^3)	3403.8(4)	4639.6(7)	3685(2)	5036(2)
a (Å)	9.5505(6)	10.881(1)	13.905(3)	18.786(4)
b (Å)	22.928(1)	22.638(2)	18.632(5)	15.301(3)
c (Å)	16.228(1)	18.839(2)	14.527(4)	17.521(4)
α (deg)	90	90	90	90
β (deg)	106.688(2)	91.090(2)	101.739(6)	90
γ (deg)	90	90	90	90
Z	4	4	2	4
fw (g/mol)	786.7	997.08	1496.7	1075.8
density (calcd) (Mg/m^3)	1.535	1.427	1.349	1.419
abs coeff (mm^{-1})	4.805	3.542	2.471	3.474
F_{000}	1560	2016	1542	2152
total no. of reflns	28403	25197	26971	36477
unique reflns	6864	9259	6853	5302
final R indices [$I > 2\sigma(I)$]	R1 = 0.045, wR2 = 0.101	R1 = 0.040, wR2 = 0.083	R1 = 0.081, wR2 = 0.178	R1 = 0.040, wR2 = 0.109
largest diff peak and hole (e/Å^3)	4.65 and −1.48	2.88 and −0.77	1.73 and −2.19	2.73 and −1.06
GOF	1.027	0.824	0.861	0.972

UO_2(Ar$_2$nacnac)(hfac) (3). To a stirring THF solution (3 mL) containing [UO_2(Ar$_2$nacnac)Cl]$_2$ (0.0361 g, 0.024 mmol) was added Na(hfac) (0.0123 g, 0.053 mmol). This resulted in the immediate formation of a deep-green solution. After stirring for 20 min, the volatiles were removed in vacuo and the resulting oil was dissolved in hexanes (3 mL). This solution was filtered through a Celite column supported on glass wool (0.5 cm × 2 cm), and the volume was reduced in vacuo to 1 mL. This solution was stored at −25 °C for 24 h to provide black crystals, which were isolated and dried in vacuo (23.6 mg, 53% yield). Anal. Calcd for $C_{34}H_{42}F_6N_2O_4U$: C, 45.64; H, 4.73; N, 3.13. Found: C, 46.78; H, 4.90; N, 2.97. ^{1}H NMR (C_6D_6, 25 °C, 500 MHz): δ 0.90 (d, 12H, J_{HH} = 6.5 Hz, CHMe_2), 1.08 (d, 12H, J_{HH} = 6.5 Hz, CHMe_2), 1.99 (s, 6H, Me), 3.58 (septet, 4H, J_{HH} = 6.5 Hz, CHMe$_2$), 4.76 (s, 1H), 6.06 (s, 1H), 7.25 (t, 2H, J_{HH} = 7.0 Hz, p-CH), 7.32 (d, 4H, J_{HH} = 7.5 Hz, m-CH). ^{19}F{^{1}H} NMR (C_6D_6, 25 °C, 376 MHz): δ −12.7 (s). ^{13}C{^{1}H} NMR (C_6D_6, 25 °C, 125 MHz): δ 23.7 (CHMe_2), 26.5 (CHMe_2), 27.3 (Me), 28.3 (CHMe_2), 93.5 (γ-C), 98.61 (γ-C), 125.8, 131.0, 131.6, 150.3 (C ipso), 166.5 (β-CN), 181.1 (β-CO). UV/vis (CH_2Cl_2, 3.7 × 10^{-4} M): 680 nm (ε = 580 L·mol^{-1}·cm^{-1}), 608 nm (sh, ε = 760 L·mol^{-1}·cm^{-1}). UV/vis (CH_2Cl_2, 4.5 × 10^{-5} M): 329 nm (ε = 21 600 L·mol^{-1}·cm^{-1}), 307 nm (ε = 22 100 L·mol^{-1}·cm^{-1}). IR (KBr pellet, cm^{-1}): 1570(s), 1563(s), 1530(s), 1404(vs), 1388(vs), 1369(s), 1317(s), 1256(vs), 1214(vs), 1150(vs), 1105(s), 1060(w), 1020(m), 932(vs), 922(vs, ν_{asy}(U═O)), 832(w), 795(s), 762(m), 743(w), 659(m), 627(w), 585(m), 430(m).

[Cp*$_2$Co][UO_2(Ar$_2$nacnac)(acac)] (4). To a toluene solution (2 mL) of **1** (0.0487 g, 0.062 mmol) was added an Et_2O solution (1 mL) of Cp*$_2$Co (0.0229 g, 0.070 mmol). A orange-red powder quickly formed at the interface of the two solutions. Storage of this mixture at −25 °C for 24 h resulted in the deposition of an orange-red crystalline powder, which was isolated by decanting off the supernatant and dried in vacuo (0.0672 g, 91% yield). Anal. Calcd for $C_{54}H_{78}CoN_2O_4U$: C, 58.11; H, 7.04 N, 2.51. Found: C, 58.31; H, 6.77; N, 2.15. ^{1}H NMR (CD_2Cl_2, 25 °C, 400 MHz): δ −7.96 (s, 6H, Me), −5.37 (s, 6H, Me), −2.17 (s, 1H, γ-CH), −0.99 (s, 12H, CHMe_2), 1.99 (s, 30H, C_5Me_5), 2.54 (s, 4H, CHMe$_2$), 2.98 (s, 4H, m-CH), 3.41 (s, 12H, CHMe_2), 4.07 (s, 2H, p-CH). One γ-CH resonance was not observed. UV/vis (CH_2Cl_2, 2.3 × 10^{-3} M): 791 nm (ε = 75 L·mol^{-1}·cm^{-1}), 644 nm (sh, ε = 210 L·mol^{-1}·cm^{-1}), 503 nm (sh, ε = 510 L·mol^{-1}·cm^{-1}). UV/vis (CH_2Cl_2, 5.0 × 10^{-5} M): 373 nm (sh, ε = 9400 L·mol^{-1}·cm^{-1}), 350 nm (sh, ε = 13 200 L·mol^{-1}·cm^{-1}). IR (KBr pellet): 1604(m), 1554(s), 1519(vs), 1435(vs), 1397(vs), 1320(s), 1270(m), 1233(w), 1170(m), 1104(w), 1022(s), 973(w), 933(w), 896(m), 838(m, ν_{asy}(U═O)), 789(m), 760(m), 636(w), 447(m).

[Cp*$_2$Co][UO_2(Ar$_2$nacnac)(dbm)] (5). To a Et_2O solution (2 mL) of **2** (0.0499 g, 0.055 mmol) was added a hexanes solution (1 mL) of Cp*$_2$Co (0.0177 g, 0.054 mmol). A tan powder quickly formed at the interface of the two solutions. Storage of this mixture at −25 °C for 24 h resulted in the deposition of a tan powder, which was isolated by decanting off the supernatant and dried in vacuo (0.0307 g, 45% yield). Anal. Calcd for $C_{64}H_{82}CoN_2O_4U$: C, 61.98; H, 6.66; N, 2.26. Found: C, 60.04; H, 6.85; N, 2.12. ^{1}H NMR (CD_2Cl_2, 25 °C, 400 MHz): δ −5.60 (s, 6H, Me), −0.77 (s, 12H, CHMe_2), 0.80 (s, 4H, aryl CH), 1.99 (s, 30H, C_5Me_5), 2.80 (s, 4H, aryl CH), 3.84 (s, 12H, CHMe_2), 4.22 (s, 4H, aryl CH), 4.60 (s, 4H, CHMe$_2$), 6.35 (s, 2H, p-CH). The γ-CH resonances and one aryl CH resonance were not observed. UV/vis (CH_2Cl_2, 1.8 × 10^{-3} M): 743 nm (ε = 170 L·mol^{-1}·cm^{-1}), 634 nm (sh, ε = 220 L·mol^{-1}·cm^{-1}), 508 nm (sh, ε = 480 L·mol^{-1}·cm^{-1}). UV/vis (CH_2Cl_2, 5.0 × 10^{-5} M): 371 nm (sh, ε = 13 600 L·mol^{-1}·cm^{-1}), 333 nm (ε = 19 000 L·mol^{-1}·cm^{-1}). IR (KBr pellet): 1599(m), 1554(m), 1521(s), 1479(s), 1464(s), 1433(m), 1393(s), 1319(m), 1228(w), 1168(m), 1104(w), 1075(w), 1066(w), 1025(m), 935(w), 910(m), 894(m), 844(m, ν_{asy}(U═O)), 793(m), 760)(m), 724(m), 693(w), 607(w), 526(w), 445(m).

[Cp*$_2$Co][UO_2(Ar$_2$nacnac)(hfac)] (6). To a toluene solution (1 mL) of **3** (0.0297 g, 0.033 mmol) was added a hexanes solution (2 mL) of Cp_2Co (0.0071 g, 0.037 mmol). Storage of this mixture at −25 °C for 24 h resulted in the deposition of an orange powder, which was rinsed with pentane (5 mL) and dried in vacuo (0.0128 g, 33% yield). Anal. Calcd for $C_{44}H_{52}CoF_6N_2O_4U$·C_7H_8: C, 52.09; H, 5.14; N, 2.38. Found: C, 51.50; H, 5.11; N, 2.05. ^{1}H NMR (CD_2Cl_2, 25 °C, 400 MHz): δ −33.9 (br s, 12H, CHMe_2), −2.05 (s, 6H, Me), −0.02 (s, 12H, CHMe_2), 2.62 (s, 1H, γ-CH), 2.75 (s, 10H, C_5H_5), 3.03 (s, 4H, CHMe$_2$), 4.68 (d, 4H, J_{HH} = 6.5 Hz, m-CH), 5.52 (t, 2H, J_{HH} = 7.0 Hz, p-CH). One γ-CH resonance was not observed. ^{19}F{^{1}H} NMR (C_6D_6, 25 °C, 376 MHz): δ −10.1 (br s). UV/vis (CH_2Cl_2, 2.1 × 10^{-3} M): 677 nm (ε = 430 L·mol^{-1}·cm^{-1}). UV/vis (CH_2Cl_2, 1.5 × 10^{-4} M): 507 nm (sh, ε = 740 L·mol^{-1}·cm^{-1}). IR (KBr pellet): 1671(s), 1556(s), 1531(s), 1465(m), 1434(s), 1415(vs), 1366(m), 1319(m), 1251(s), 1187(s), 1172(s), 1148(s), 1127(s), 1068(w), 1031(m), 936(w),

864(s,ν_{asy}(U═O)), 842(sh), 791(m), 759(w), 766(w), 697(w), 660(m), 572(w), 464(s).

[NEt_4][UO_2(Ar_2nacnac)(Me(O)CHC(O)═CH_2)] (7). Method A. To a stirring THF solution (3 mL) containing UO_2(Ar_2nacnac)(acac) (0.0253 g, 0.032 mmol) was added sodium (0.0021 g, 0.09 mmol). After stirring for 2 h, the excess sodium was removed, [NEt_4]Cl (0.0068 g, 0.041 mmol) was added to the reaction mixture, and stirring was continued for another 30 min. This mixture was filtered through a Celite column supported on glass wool (0.5 cm × 2 cm), and the filtrate was layered with an equal volume of hexanes. Storage of this solution at −25 °C for 24 h resulted in the deposition of a tan powder. This mixture was again filtered through a Celite column supported on glass wool (0.5 cm × 2 cm), and the filtrate was layered with hexanes (2 mL). This solution was stored at −25 °C for a further 24 h to provide red crystals, which were isolated and dried in vacuo (0.0035 g, 12% yield). Anal. Calcd for $C_{42}H_{67}N_3O_4U$: C, 55.07; H, 7.37; N, 4.59. Found: C, 55.38; H, 7.72; N, 4.44. ^{1}H NMR (THF-d_8, 25 °C, 400 MHz): δ 0.98 (br s, 12H, NCH_2CH_3), 1.00 (d, 6H, J_{HH} = 6.8 Hz, $CHMe_2$), 1.10 (d, 6H, J_{HH} = 6.4 Hz, $CHMe_2$), 1.17 (d, 6H, J_{HH} = 6.4 Hz, $CHMe_2$), 1.18 (d, 6H, J_{HH} = 6.8 Hz, $CHMe_2$), 1.43 (s, 3H, Me), 2.01 (s, 3H, Me), 2.02 (s, 3H, Me), 2.50 (d, 1H, J_{HH} = 2.0 Hz, C═CH), 2.84 (d, 1H, J_{HH} = 2.0 Hz, C═CH), 2.99 (br s, 8H, NCH_2CH_3), 3.69 (septet, 2H, J_{HH} = 6.8 Hz, $CHMe_2$), 3.74 (septet, 2H, J_{HH} = 6.4 Hz, $CHMe_2$), 4.55 (s, 1H, γ-CH), 4.98 (s, 1H, γ-CH), 7.07−7.17 (m, 6H, overlapping CH). ^{13}C{^{1}H} NMR (THF-d_8, 25 °C, 125 MHz): δ 7.68 (NCH_2CH_3), 23.4, 23.7, 25.9, 26.0, 26.2, 27.1, 27.3, 28.4, 28.6, 52.8 (NCH_2CH_3), 80.4 (C═CH_2), 97.4 (γ-C), 101.2 (γ-C), 124.3, 126.1, 126.2, 144.3, 144.6, 146.3, 146.5, 161.5 (β-CN), 166.8 (β-CN), 186.9 (β-CO), 169.7 (β-CO).

Method B. To a stirring THF solution (3 mL) containing UO_2(Ar_2nacnac)(acac) (0.0542 g, 0.069 mmol) was added NaN($SiMe_3$)$_2$ (0.0131 g, 0.071 mmol). This resulted in the immediate formation of a deep-maroon solution. After stirring for 15 min, [NEt_4]Cl (0.0121 g, 0.073 mmol) was added to the reaction mixture and the stirring was continued for another 30 min. This mixture was filtered through a Celite column supported on glass wool (0.5 cm × 2 cm), and the filtrate was layered with an equal volume of hexanes. This solution was stored at −25 °C for 24 h to provide red crystals, which were isolated and dried in vacuo (0.0432 g, 69% yield).

X-ray Crystallography. The crystal structures of complexes **1**, **2**·C_6H_{14}, **5**·$2C_7H_8$·THF, and **7**·$2CH_2Cl_2$ were determined similarly, with exceptions noted in subsequent paragraphs. Crystals were mounted on a glass fiber under Paratone-N oil. Data collection was carried out on a Bruker 3-axis platform diffractometer with a SMART-1000 CCD detector. The instrument was equipped with a graphite-monochromatized Mo Kα X-ray source (λ = 0.710 73 Å). All data were collected at 150(2) K using an Oxford nitrogen gas cryostream system. A hemisphere of data was collected using ω scans, with 15 s (for **1**, **2**·C_6H_{14}, and **7**·$2CH_2Cl_2$) or 25 s (for **5**·$2C_7H_8$·THF) frame exposures and 0.3° frame widths. *SMART*[63] was used to determine the cell parameters and data collection. The raw frame data were processed using *SAINT*.[64] The empirical absorption correction was applied based on ψ scan. Subsequent calculations were carried out using *SHELXTL*.[65] The structures was solved using direct methods and difference Fourier techniques. All hydrogen atom positions were idealized and rode on the atom of attachment. The final refinement included anisotropic temperature factors on all non-hydrogen atoms. Structure solution, refinement, graphics, and creation of publication materials were performed using *SHELXTL* or *WinGX*.[66]

For complex **1**, C28 was refined isotropically. For complex **5**·$2C_7H_8$·THF, the C−C distances of one Cp* ring were fixed at 1.4 Å, while the C−Me distances were fixed at 1.5 Å. In addition, because of disorder, the methyl group of one toluene solvate molecule could not be located. The atoms of the disordered solvent molecules were refined isotropically, while the hydrogen atoms were typically not assigned to these carbons. For complex **7**·$2CH_2Cl_2$, the NEt_4^+ cation was found to sit on two independent special positions, with 0.25 occupancies at both positions. In addition, each cation was disordered between two orientations that were modeled using a 50:50 ratio. X-ray crystallographic data for **1**, **2**·C_6H_{14}, **5**·$2C_7H_8$·THF, and **7**·$2CH_2Cl_2$ can be found in Table 2.

Acknowledgment. We thank the University of California at Santa Barbara for financial support of this work. We also thank Dr. Alexandre Mikhailovsky for assistance with the UV/vis and fluorescence measurements.

Supporting Information Available: X-ray crystallographic details (as CIF files) of **1**, **2**·C_6H_{14}, **5**·$2C_7H_8$·THF, and **7**·$2CH_2Cl_2$, tabulated cyclic voltammetry data for **1**−**3**, and absorption and fluorescence spectra for **1**. This material is available free of charge via the Internet at http://pubs.acs.org.

IC800778J

(63) *SMART Software Users Guide*, version 5.1; Bruker Analytical X-ray Systems, Inc.: Madison, WI, 1999.
(64) *SAINT Software Users Guide*, version 5.1; Bruker Analytical X-ray Systems, Inc.: Madison, WI, 1999.
(65) Sheldrick, G. M. *SHELXTL*; Bruker Analytical X-ray Systems, Inc.: Madison, WI, 2001.
(66) Farrugia, L. J. *J. Appl. Crystallogr.* **1999**, *32*, 837–838.